

## SPACESHIP EARTH OBSERVATIONS OF THE EASTER 2001 SOLAR PARTICLE EVENT

JOHN W. BIBER, PAUL EVENSON, WOLFGANG DRÖGE, AND ROGER PYLE  
Bartol Research Institute, University of Delaware, 217 Sharp Laboratory, Newark, DE 19716

DAVID RUFFOLO,<sup>1</sup> MANIT RUJIWARODOM, AND PAISAN TOOPRAKAI  
Department of Physics, Chulalongkorn University, Bangkok 10330, Thailand

AND

THIRANEE KHUMLUMLERT

Department of Physics, Naresuan University, Science Complex, Tah Poe District, Phitsanulok 65000, Thailand

Received 2003 September 4; accepted 2003 December 4; published 2004 January 15

### ABSTRACT

The largest relativistic ( $\sim 1$  GeV) solar proton event of the current solar activity cycle occurred on Easter 2001 (April 15). This was the first such event to be observed by Spaceship Earth, an 11-station network of neutron monitors optimized for measuring the angular distribution of solar cosmic rays. We derive the particle density and anisotropy as functions of time and model these with numerical solutions of the Boltzmann equation. We conclude that transport in the interplanetary medium was diffusive in this event, with a radial mean free path of 0.17 AU. The high time resolution of the Spaceship Earth network and the fast particle speed permit accurate determination of particle injection timing at the solar source. We find that particle injection at the Sun began at 13:42 UT  $\pm 1$  minute, about 14 minutes before the first arrival of particles at Earth, in close association with the onset of shock-related radio emissions and  $\sim 15$  minutes after liftoff of a coronal mass ejection (CME). Our results are consistent with the hypothesis that solar particles were accelerated to GeV energies on Easter 2001 by a CME-driven shock wave.

*Subject headings:* acceleration of particles — solar-terrestrial relations —  
Sun: coronal mass ejections (CMEs) — Sun: flares — Sun: particle emission

### 1. INTRODUCTION

Spaceship Earth is a network of neutron monitors strategically deployed to provide real-time three-dimensional measurements of the cosmic-ray angular distribution with excellent statistics and 1 minute time resolution. As shown in Figure 1, it comprises 11 stations on four continents sited to provide good sky coverage of the equatorial region together with a three-dimensional perspective from Thule and McMurdo. The asymptotic viewing direction shown for each station is the direction from which the primary cosmic rays were coming before encountering the distorting magnetic fields of Earth's magnetosphere. The name Spaceship Earth recognizes both the multinational scope of the project (US, Russian, Australian, and Canadian participation) as well as the similarity of the measurement strategy to that employed by modern particle detectors flown in space.

Figure 2 shows count rates recorded by five selected stations of Spaceship Earth during the solar particle event of 2001 April 15. This event was so large that it increased radiation levels at Earth's surface; hence it qualifies for designation as a "ground level enhancement" (GLE). The earliest onset was recorded at 13:56 UT at Fort Smith, Canada. The minimum detected energy is 0.4 GeV and is determined by atmospheric absorption at these high-latitude sites; the geomagnetic cutoff is below this and plays no role. Thus, all Spaceship Earth neutron monitors have the same energy response, and the differing time profiles in Figure 2 result from anisotropy of the particle angular distribution. Stations with a favorable viewing direction (e.g., Nain and Fort Smith) exhibit a rapid rise and comparatively high peak. Owing to scattering by magnetic turbulence in the interplanetary medium, however, even stations

with an unfavorable viewing direction (e.g., Apatity) measure finite particle intensity.

### 2. MODELING RESULTS

The full power of Spaceship Earth is realized when the individual stations are analyzed in concert and the network itself becomes the observing instrument. For this event, we found that a simple first-order anisotropy provides a good description of the cosmic-ray angular distribution. Network data were fitted to the function

$$f(\theta, \phi) = n(1 + \xi_x \sin \theta \cos \phi + \xi_y \sin \theta \sin \phi + \xi_z \cos \theta), \quad (1)$$

where  $f(\theta, \phi)$  is the intensity measured by a station with an asymptotic viewing direction defined by  $\theta$  (colatitude) and  $\phi$  (longitude),  $n$  is the particle density, and  $(\xi_x, \xi_y, \xi_z)$  are the three components of the anisotropy vector.

Results of the first-order fit appear as data points in Figure 3. The second panel displays the cosmic-ray density expressed as a percentage of the preevent background of Galactic cosmic rays. The bottom two panels display two representations of the anisotropy, the "weighted anisotropy" defined as  $n\xi$  and the ordinary anisotropy defined as  $\xi = (\xi_x^2 + \xi_y^2 + \xi_z^2)^{1/2}$ .

The solid lines in Figure 3 represent a fit of the Spaceship Earth data to a theoretical model. Specifically, the density and weighted anisotropy in the second and third panel were modeled with numerical solutions of the Boltzmann equation (Roelof 1969; Ruffolo 1995) using the method of least squares. (The temporary suppression of weighted anisotropy from 14:17 to 14:32 UT is apparently a localized effect that cannot be described by our model; hence this interval was omitted from the fitting procedure.) Modeling the density and anisotropy to-

<sup>1</sup> Current address: Department of Physics, Faculty of Science, Mahidol University, Rama VI Road, Bangkok 10400, Thailand.

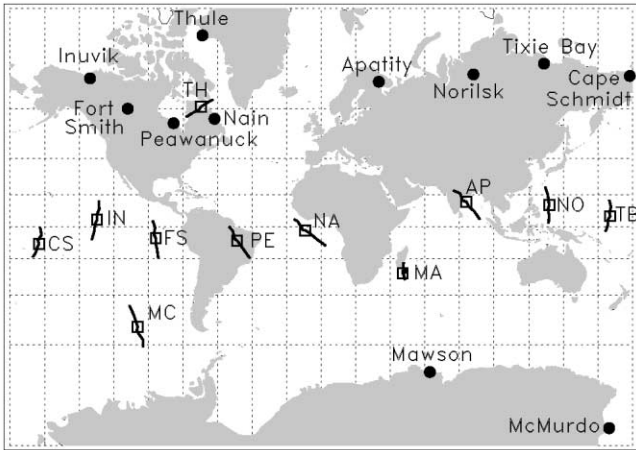


FIG. 1.—SpacESHip Earth neutron monitor network. All stations (filled circles) are at high geographic latitudes, but nine of them view the equatorial region after accounting for bending of particle trajectories in the geomagnetic field, while Thule and McMurdo generally view the northern and southern hemispheres, respectively. Squares show asymptotic (see text) viewing directions for a median energy particle (1.3 GeV for this event), and the lines show the range of viewing directions for the central 50% of the detector energy response (0.7–2.3 GeV for this event). Two-letter station codes correspond to the first two letters of the station name or the first letter of each word in the case of a two-word name. Asymptotic directions were computed with the aid of a trajectory code (Lin, Bieber, & Evenson 1995) for a time near the start of the Easter 2001 solar cosmic-ray event.

gether is crucial for deriving the particle injection profile—otherwise, effects of prolonged injection could not be separated from diffusive delays in the interplanetary medium. The anisotropy contains key information on the strength of scattering in the interplanetary medium.

The free parameters of the fit were the radial mean free path, which was taken to be constant as a function of radius, and several parameters<sup>2</sup> describing a piecewise linear “injection function,” defined as the rate at which particles are injected onto the solar footpoint of the Sun–Earth magnetic field line as a function of time (Ruffolo, Khumlumert, & Youngde 1998).

The derived injection function is shown in the top panel of Figure 3. The best-fit radial mean free path is 0.17 AU, which corresponds nominally to a parallel mean free path of 0.34 AU at Earth. Results from the  $\chi^2$  minimization method employed here are compatible with those obtained by the traditional technique of matching density and anisotropy profiles by eye (Bieber et al. 2002).

### 3. SPECTRUM PARAMETER

According to the quasilinear theory of particle scattering, particle transport also depends on the spectrum of the scattering turbulence (Jokipii 1966). Typically this is described via a spectral index  $q$  of an assumed power-law dependence of the one-dimensional magnetic power spectrum,  $P(k) \propto |k|^{-q}$ , where  $k$  is the wavenumber of the turbulence mode. The model results in Figure 3 used  $q = 1$ . Although turbulence in interplanetary space often has a Kolmogoroff form ( $q = 5/3$ ) at smaller scales, there are reports of a possible shallower index at the large scales responsible for scattering particles of neutron monitor energy (Matthaeus & Goldstein 1982; Bieber & Pomerantz 1983; Bieber et al. 1993).

<sup>2</sup> The piecewise linear injection function is described by 5 amplitudes  $a_i$  at joint times  $t_i$ , where  $t_i = t_0 + 2^{i-1}\tau$  are specified by  $t_0$  and  $\tau$ .

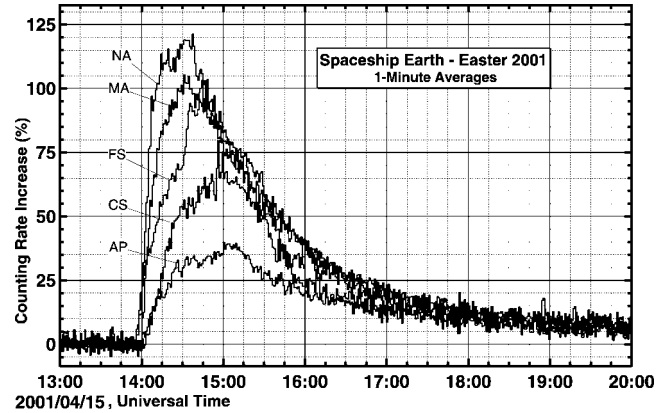


FIG. 2.—Neutron rates recorded at selected SpacESHip Earth stations during the GLE of Easter 2001. All stations are shown at a time resolution of 1 minute. The detected neutrons are secondary cosmic rays generated by cascades in Earth’s atmosphere. The primary cosmic rays initiating the cascades are predominantly protons. See Fig. 1 for definition of two-letter station codes.

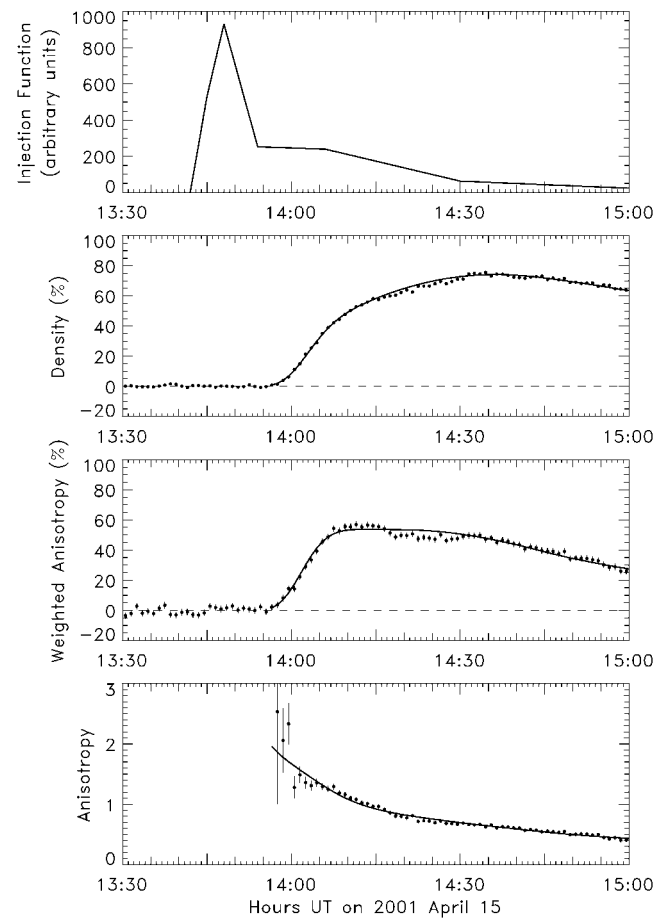


FIG. 3.—Data points (bottom three panels) show solar cosmic-ray density, weighted anisotropy, and anisotropy derived by fitting SpacESHip Earth data to a first-order anisotropy. Curves show predictions of a model based on numerical solution of the Boltzmann equation with a best-fit radial mean free path of 0.17 AU and with the injection function shown in the top panel. The  $\chi^2$  statistic is 110 with 90 degrees of freedom, indicating a good fit.

We did not attempt to optimize the model with respect to the index  $q$ , but we did compare results obtained for  $q = 1.0$  with those obtained for  $q = 1.5$ . Figure 4 displays selected 1 minute pitch-angle distributions along with model predictions for the two values of  $q$ . The theoretical curves are those implicit in the fits to the time profiles of density and weighted anisotropy in Figure 3; no additional free parameters were introduced in making the comparison shown in Figure 4.

Although the difference is not visually dramatic, we conclude that the  $q = 1.0$  fits generally provide a better description of the observations than  $q = 1.5$ . For the interval 13:56–15:00 UT,  $q = 1.0$  provides the better fit for 53 out of 64 available 1 minute samples, as determined by a  $\chi^2$  test. Summing over the entire interval, the Fisher  $F$ -statistic (Bevington & Robinson 2003) has a value of 1.2994 (ratio of  $q = 1.5$  to  $q = 1.0$ ) for 444 degrees of freedom, indicating with 99.7% confidence that  $q = 1.0$  yields a significantly better fit. This justifies our use of  $q = 1.0$  for modeling the Easter GLE. Further, the radial mean free path and injection onset are not very sensitive to  $q$ ; with  $q = 1.5$  the radial mean free path increases to 0.18 AU, and the injection onset is 1 minute earlier.

#### 4. PARTICLE INJECTION ONSET

One of the key features of Spaceship Earth observations combined with detailed modeling of the data is that injection onset times can be determined with unprecedented precision. (The high particle speed and relatively large mean free paths also contribute.) We conclude that the onset of particle injection onto the Sun-Earth field line was at 13:42 UT  $\pm$  1 minute. First detection of particles at Earth was 14 minutes later, implying that the particles traveled a total path length of 1.7 AU in the interplanetary medium. In contrast, that travel time would be  $\sim$ 10 minutes and the path length  $\sim$ 1.2 AU in the case of scatter-free propagation along the spiral magnetic field line. According to our model, scattering by magnetic turbulence in the interplanetary medium is the cause of the extra 0.5 AU in path length and the extra 4 minutes of travel time.

There is now compelling evidence that particles of MeV energies from large gradual solar events (such as the Easter 2001 event) are accelerated by shock waves driven by coronal mass ejections (CMEs; Reames 1999). However, the case for shock acceleration to GeV energies is less firmly established (but see Pomerantz & Duggal 1974 and Levy, Duggal, & Pomerantz 1976). Comparison of the precise injection onset determined from Spaceship Earth with solar radio and optical data reveals clues to the acceleration site and mechanism (cf. Tylka et al. 2002, 2003; Gopalswamy et al. 2002).

An X14.4 soft X-ray event began at 13:11 ST and peaked at 13:42 ST.<sup>3</sup> (Note that in this discussion, we report time of emission at the Sun, which we designate “ST.” For electromagnetic radiation, ST is simply the Universal Time of observation minus the 8 minute travel time.) Hard X-rays were emitted starting at 13:28 ST. H $\alpha$  emission from a flare located at S20 W85 began at 13:28 ST and peaked at 13:41 ST. Type III radio emission<sup>4</sup> due to energetic electrons began at 13:36 ST. Radio burst onsets signifying the formation of a shock wave occurred at 13:40 ST (type II) and 13:44 ST (type IV). CME

<sup>3</sup> Timing information for solar radio, optical, and soft X-ray data is available on-line from the Space Environment Center. The URL for the Easter event listing is [http://solar.sec.noaa.gov/ftpdir/indices/2001\\_events/20010415events.txt](http://solar.sec.noaa.gov/ftpdir/indices/2001_events/20010415events.txt). Timing information for hard X-rays is from *Yohkoh*/hard X-ray telescope and is available online at <http://www.lmsal.com/SXT>.

<sup>4</sup> The frequency range of all radio data mentioned here is 30–80 MHz.

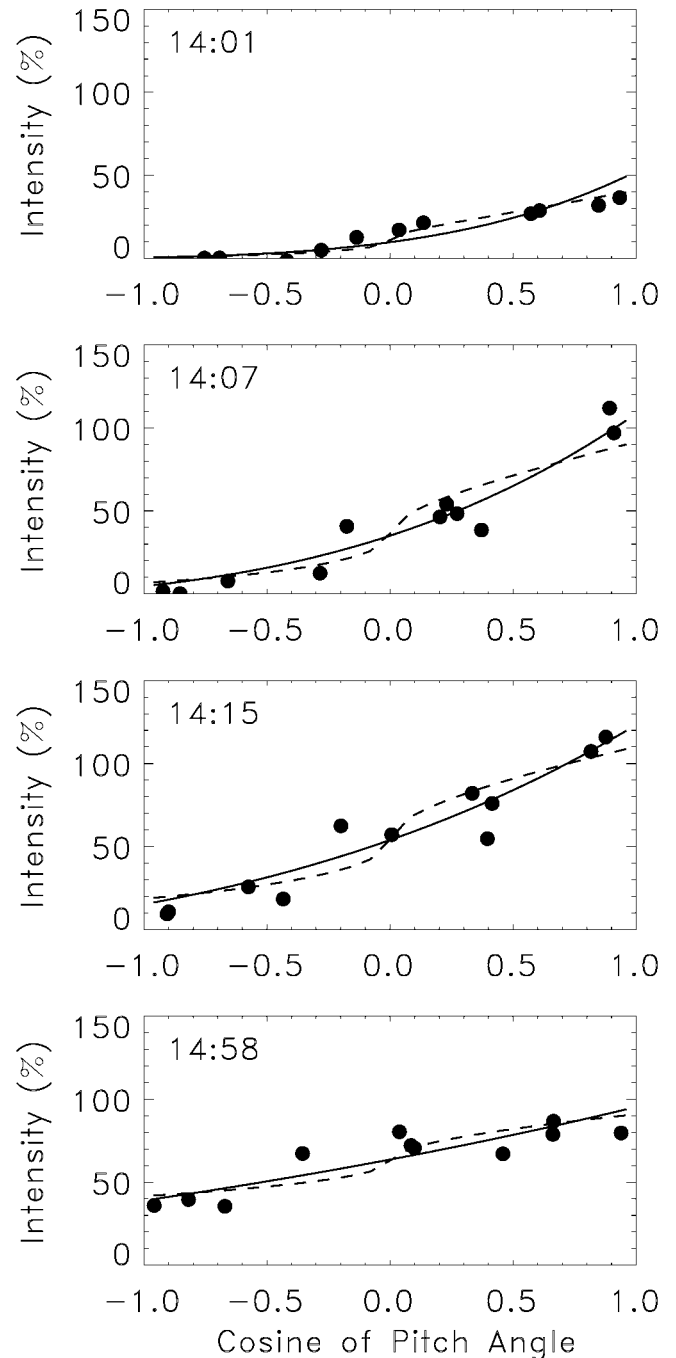


FIG. 4.—Selected 1 minute pitch-angle distributions compared with model predictions for  $q = 1.0$  (solid line) and  $q = 1.5$  (dashed line). Each data point represents the intensity recorded by an individual Spaceship Earth station for the UT minute starting at the time shown in the top left of each panel. Pitch angle is the angle between the station asymptotic viewing direction and the symmetry axis determined from the first-order fit to the data.

liftoff is estimated to have occurred between 13:24 ST (linear fit) and 13:31 ST (quadratic fit).<sup>5</sup> From the start of particle injection at 13:42 ST until the end of the interval shown in

<sup>5</sup> Source: *Solar and Heliospheric Observatory (SOHO)*/Large Angle and Spectrometric Coronagraph Experiment CME catalog, available on the Web at [http://cdaw.gsfc.nasa.gov/CME\\_list](http://cdaw.gsfc.nasa.gov/CME_list). This CME catalog is generated and maintained by NASA and Catholic University of America in cooperation with the Naval Research Laboratory. *SOHO* is a project of international cooperation between ESA and NASA.

Figure 3, the CME moved from a height of approximately 2 solar radii above the solar surface to approximately 10 solar radii above the solar surface.<sup>6</sup>

## 5. DISCUSSION

In summary, flare onset in the Easter 2001 event was at 13:11 ST (onset of soft X-ray emission), CME liftoff was between 13:24 and 13:31 ST, and particle injection onset was at 13:42 ST. The particle onset is only 2.6 minutes earlier than that reported by Tylka et al. (2003) using the inverse velocity method, but we believe that our onset is the more reliable because it is based on a more complete treatment of interplanetary transport. Since the CME release and flare onset both preceded the particle injection onset, acceleration in the flare or by a CME shock are both possible sources for the GeV solar particles observed on Easter 2001. Nonetheless, the onset timing would tend to favor shock acceleration, because (1) the particle injection onset is closer in time to the CME liftoff than the flare onset (~15 vs. 31 minutes), and (2) the particle injection onset is accompanied by shock-associated radio signatures.

Our modeling has yielded not only the particle injection onset but also a detailed time profile of the injection process (Fig. 3, *top panel*). The shape of this profile is presumably determined by details of the acceleration process and possible transport processes in the solar corona. Modeling these processes is beyond the scope of this Letter, but we invite researchers in flare acceleration and shock acceleration to attempt to explain this profile with their models.

<sup>6</sup> See figure at [http://cdaw.gsfc.nasa.gov/CME\\_list/UNIVERSAL/2001\\_04/htpng/20010415.140631.p268g.htm](http://cdaw.gsfc.nasa.gov/CME_list/UNIVERSAL/2001_04/htpng/20010415.140631.p268g.htm).

Our modeling of particle pitch-angle distributions in the Easter event has also provided information on the “ $q$ ” parameter, which according to scattering theory is linked to the slope of the magnetic power spectrum (Jokipii 1966). Specifically we found that a value  $q = 1$  provides a better fit to the data than  $q = 1.5$ . This is somewhat surprising, because 2 GV particles are typically resonant with the low end of the turbulence inertial range, where a slope near the Kolmogoroff value,  $q = 5/3$ , might be expected. [Specifically, the resonant wavenumber is  $k_{\text{res}} = (R_L \cos \theta)^{-1}$ , where  $R_L$  and  $\theta$  are the particle Larmor radius and pitch angle. In this event, we estimate  $k_{\text{res}} > 10^{-6} \text{ km}^{-1}$ , whereas the inertial range would typically begin at 5 times lower wavenumber,  $k = 2 \times 10^{-7} \text{ km}^{-1}$ .] Indeed, pitch-angle distributions in the Bastille Day event do exhibit a rapid variation near  $90^\circ$  pitch angle, which is characteristic of the higher  $q$  values (see Fig. 12 of Bieber et al. 2002).

However, a preliminary analysis of *Wind* Magnetic Fields Investigation magnetic field data for the Easter event does reveal an unusual spectral break at  $k = 10^{-5} \text{ km}^{-1}$ , with a spectral index of  $q = 1.3$  below and  $q = 1.8$  above this value. This is qualitatively in accord with our result of a low  $q$ -value in the Easter event.

We thank R. Schwenn for a useful discussion. We thank our colleagues at IZMIRAN (Russia), Polar Geophysical Institute (Russia), and Australian Antarctic Division for furnishing data. This work was supported by the US National Science Foundation under grant ATM-0000315, by the Thailand Research Fund, and by the Rachadapisek Sompoj Fund of Chulalongkorn University.

## REFERENCES

- Bevington, P. R., & Robinson, D. K. 2003, *Data Reduction and Error Analysis for the Physical Sciences* (3d ed.; Boston: McGraw Hill)
- Bieber, J. W., Chen, J., Matthaeus, W. H., Smith, C. W., & Pomerantz, M. A. 1993, *J. Geophys. Res.*, 98, 3585
- Bieber, J. W., & Pomerantz, M. A. 1983, *Geophys. Res. Lett.*, 10, 920
- Bieber, J. W., et al. 2002, *ApJ*, 567, 622
- Gopalswamy, N., Yashiro, S., Kaiser, M. L., & Howard, R. A. 2002, *Adv. Space Res.*, in press
- Jokipii, J. R. 1966, *ApJ*, 146, 480
- Levy, E. H., Duggal, S. P., & Pomerantz, M. A. 1976, *J. Geophys. Res.*, 81, 51
- Lin, Z., Bieber, J. W., & Evenson, P. 1995, *J. Geophys. Res.*, 100, 23,543
- Matthaeus, W. H., & Goldstein, M. L. 1982, *Phys. Rev. Lett.*, 57, 495
- Pomerantz, M. A., & Duggal, S. P. 1974, *J. Geophys. Res.*, 79, 913
- Reames, D. V. 1999, *Space Sci. Rev.*, 90, 413
- Roelof, E. C. 1969, in *Lectures in High Energy Astrophysics*, ed. H. Ögelmann & J. R. Wayland (NASA SP-199; Washington, DC: NASA), 111
- Ruffolo, D. 1995, *ApJ*, 442, 861
- Ruffolo, D., Khumlumert, T., & Youngde, W. 1998, *J. Geophys. Res.*, 103, 20,591
- Tylka, A. J., Boberg, P. R., Cohen, C. M. S., Dietrich, W. F., MacLennan, C. G., Mason, G. M., Ng, C. K., & Reames, D. V. 2002, *ApJ*, 581, L119
- Tylka, A. J., et al. 2003, *Proc. 28th Int. Cosmic Ray Conf.* (Tsukuba), 3305